Lecture 26 - Quasar Absorption Lines

1. Introduction
2. Basics
3. Absorption Line Classes
4. Damped Lyα Systems

References

Osterbrock & Ferland, Chs 13-14

Graham, Ay216 Lec15-2005

Wolfe et al. ARAA 43 861 2005

Discovery of Quasars

Quasi-Stellar Objects, QSOs, or quasars were first identified by by Maartin Schmidt in 1963 with the 200-inch Palomar telescope

- 3C273, the first quasar has redshift of $z = 0.15$

Osterbrock traces AGN history to Fath (Lick Obs. 1908), who detected emission lines in NGC 1068.

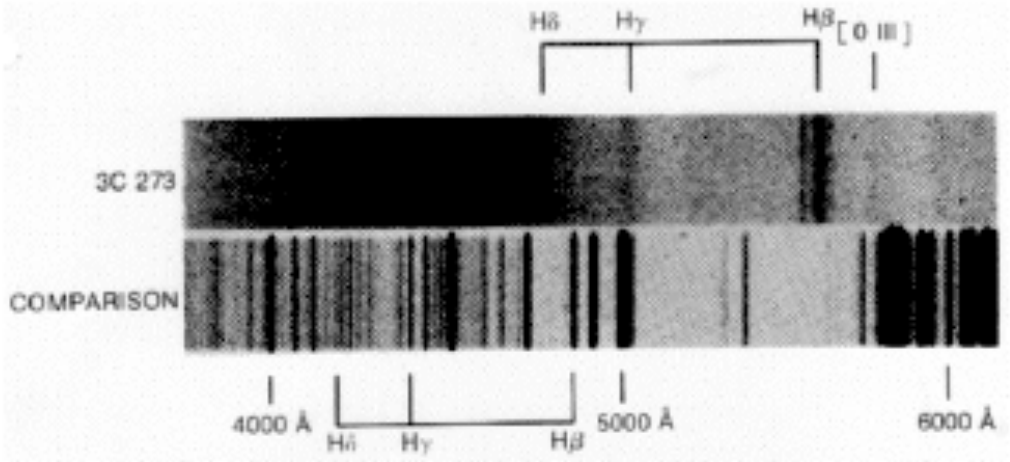

- The highest known redshift quasar has $z = 6.4$

QSO absorption lines were discovered within few years of the identification of 3C273

Quasars and Their Spectra

Luminous sources (up to > 10^{12} L_{sun}) at galactic centers:

- featureless continua extending from radio to X-rays
- strong nebular emission lines up to z_{em} ~ 6
- rich absorption line spectra (slide 5)

Composite rest frame spectrum of 2204 SDSS quasars with power-law (black hole) continuum and strong emission lines (c.f. irradiation of circum-blackhole gas).

• Our concern here is not with the origin of the emission lines: see Chs. 13-14 of Osterbrock & Ferland.

• AGN come in many types, and quasars are the most powerful and most useful beacons.

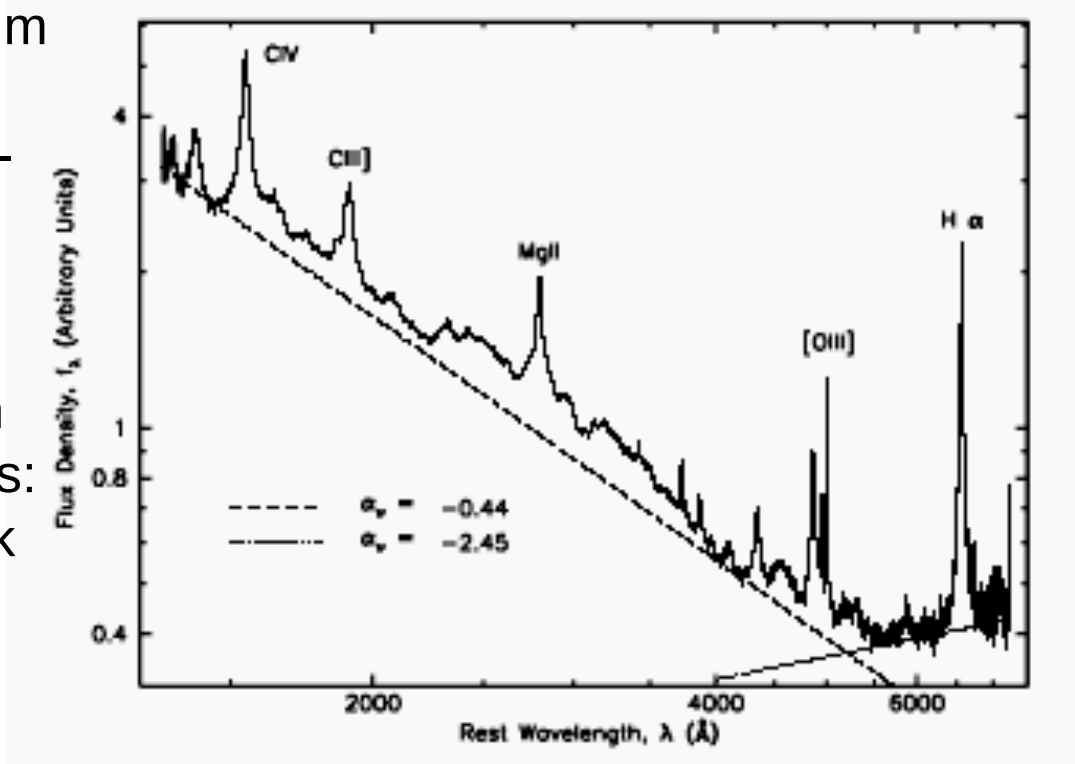

Vander Berk et al. AJ 122 549 2001

Redshift Distribution of SDSS Quasars

- The few quasars above $z = 2$ are particularly important because they probe farr back in time and distance.
- Finding more quasars $z > 6$ is an important goal.

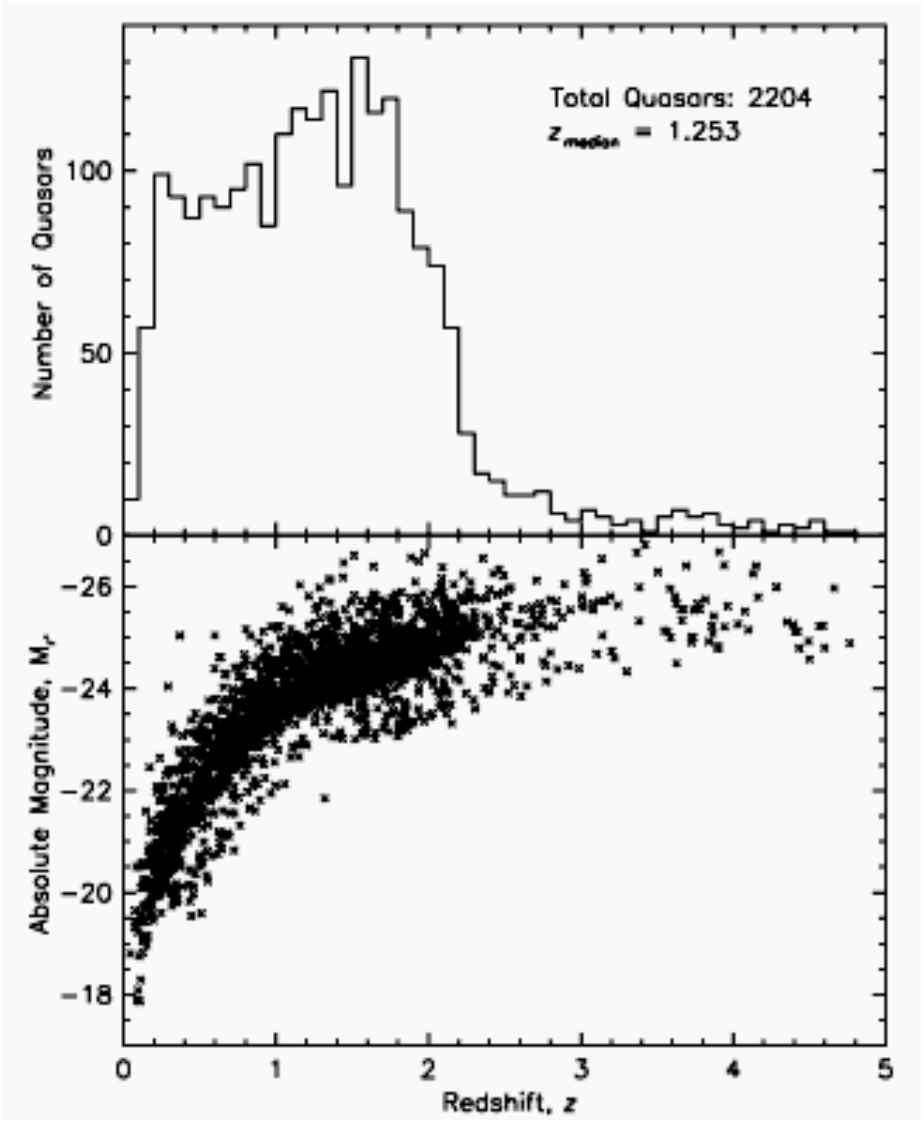

2204 quasars with median $z = 1.253$

Quasars as Probes of Intervening Matter

Quasar radiation is absorbed mainly along the entire line of sight of the “inter-galactic medium” (IGM), including intervening galaxies and the ISM of the Milky Way.

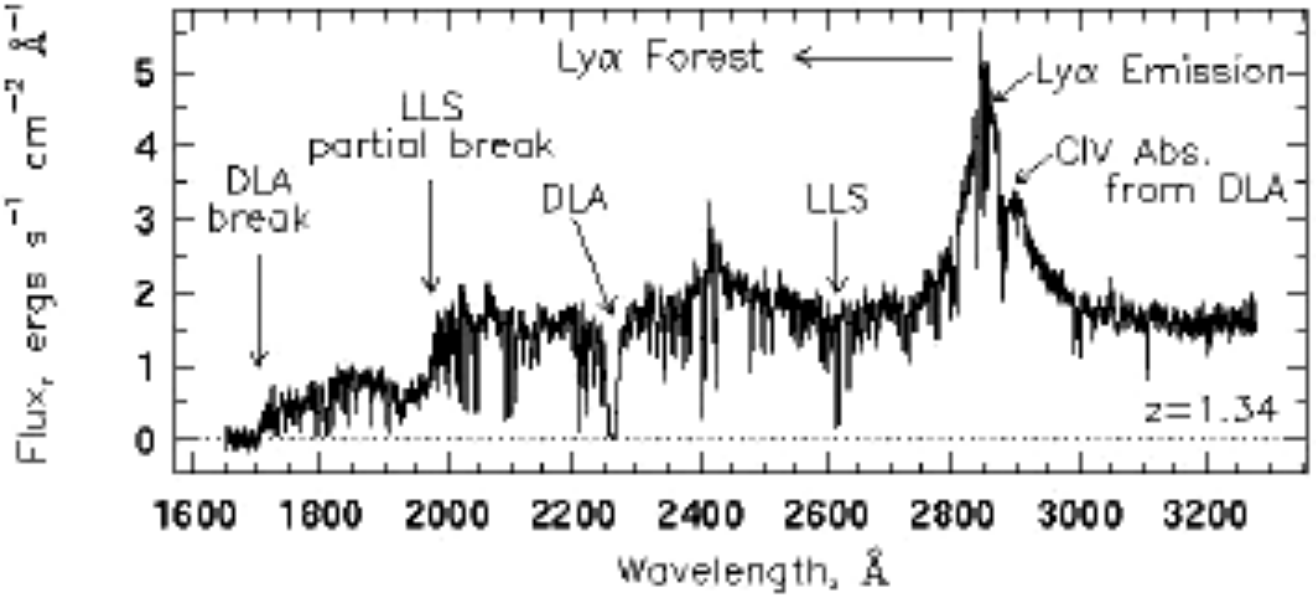

PKS 0454+0339, z = 1.34

Typical moderate-z quasar spectrum showing the dominant Lyα emission line and many absorption lines, especially many Lyα.

Some Cosmological Background

Concordance Cosmological Parameters

based on all relevant observations, e.g., CBR, SNRs,etc.

$$\Omega_i = \frac{\rho_i}{\rho_{cr}} \qquad \rho = \rho_\Lambda + \rho_{DM} + \rho_B$$

$$\rho_{cr} = \frac{3H_0^{\,2}}{8\pi G} = h^2\, 1.88 \times 10^{-29}\ \mathrm{gr\ cm^{-3}} \qquad H_0 = h\ \ 100\ \mathrm{km\ s^{-1} Mpc^{-1}}$$

$$h = 0.70 \qquad \Omega_\Lambda = 0.73 \quad \Omega_{DM} = 0.22 \qquad \Omega_B = 0.04$$

Observed wavelengths are shifted from the rest value according to the redshift *z* of the source of the radiation.

$$\lambda = \lambda_0 (1 + z)$$

Redshift as Lookback Time

$$t = \frac{t_n}{(1+z)^{3/2}} \qquad t_n \cong 13.73\,\mathrm{Gyr}$$

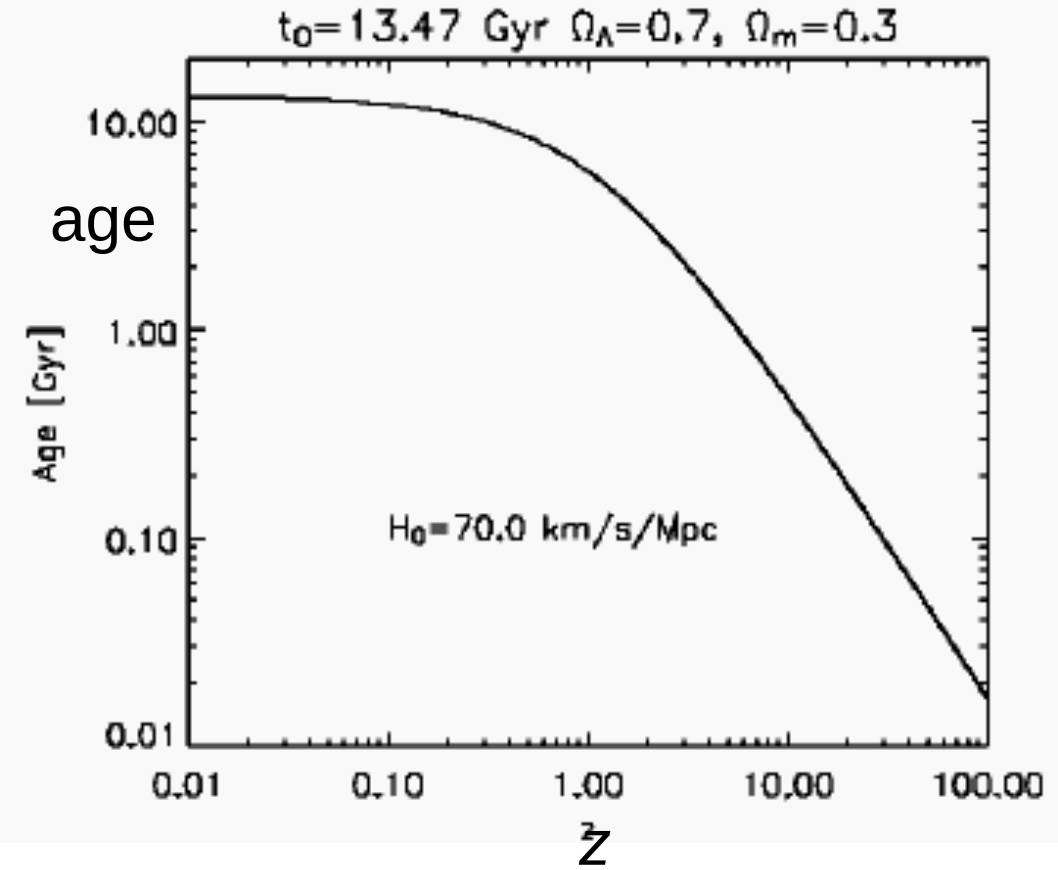

2. Basis of Quasar Absorption Spectroscopy

- The spectra are complex and many of the lines are weak
- The observations are done with large ≥ 4m telescopes at high resolution, e.g., R=45,000 for Keck HIRES
- The methodology for the analysis of the lines is the same as for ISM absorption lines based on the absorption cross section

$$\sigma_{lu}(\nu) = f_{lu} \frac{\pi e^2}{m_e c} \phi_{lu}(\upsilon)$$

with the Voigt line profile

$$\phi(\nu) = \frac{1}{\sqrt{\pi} b} \int_{-\infty}^{\infty} e^{-(w/b)^2} \frac{1}{\pi} \frac{\gamma_k}{\gamma_k^2 + (\Delta\nu + \nu_0 w/c)^2} dw$$

Variation of Lyα with *N*(HI) and Doppler *b*

Vary *N*(HI)

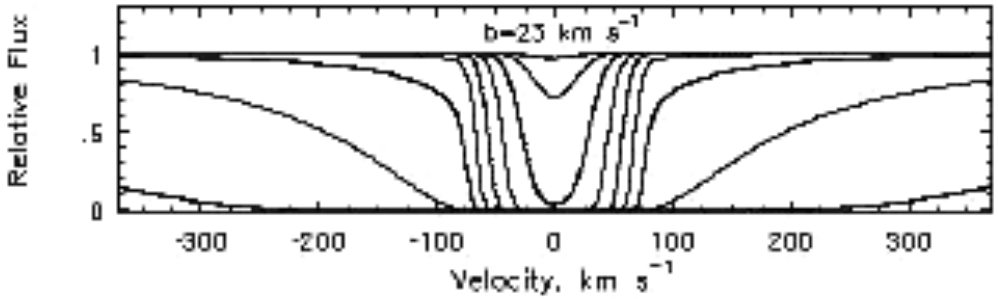

Vary *N*(HI) and *b*

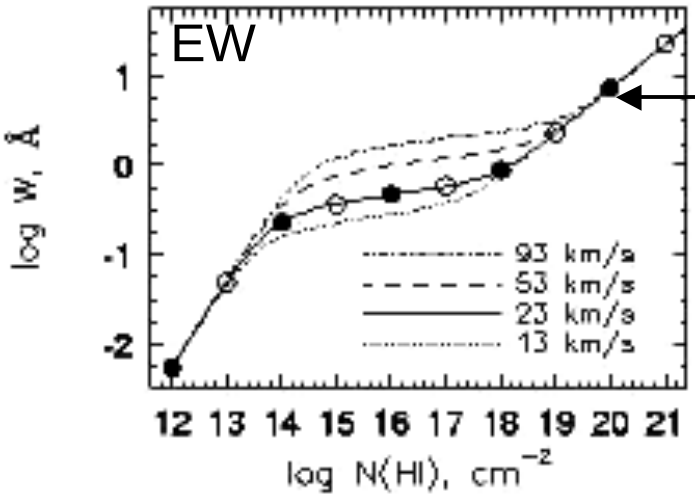

square root or "damping" part of the curve of growth

Vary *b*

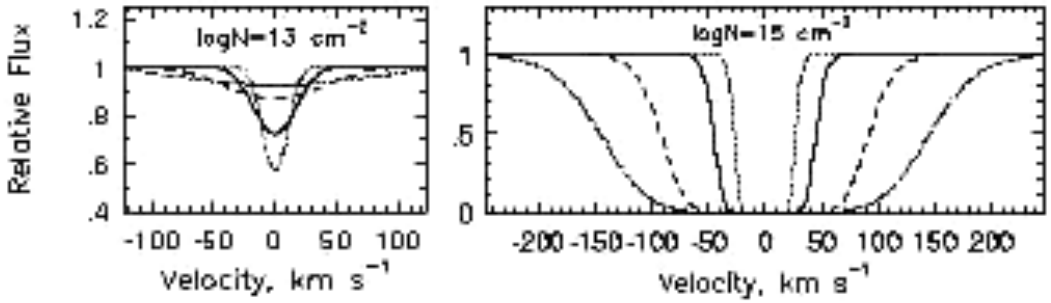

QSO Absorption Line System

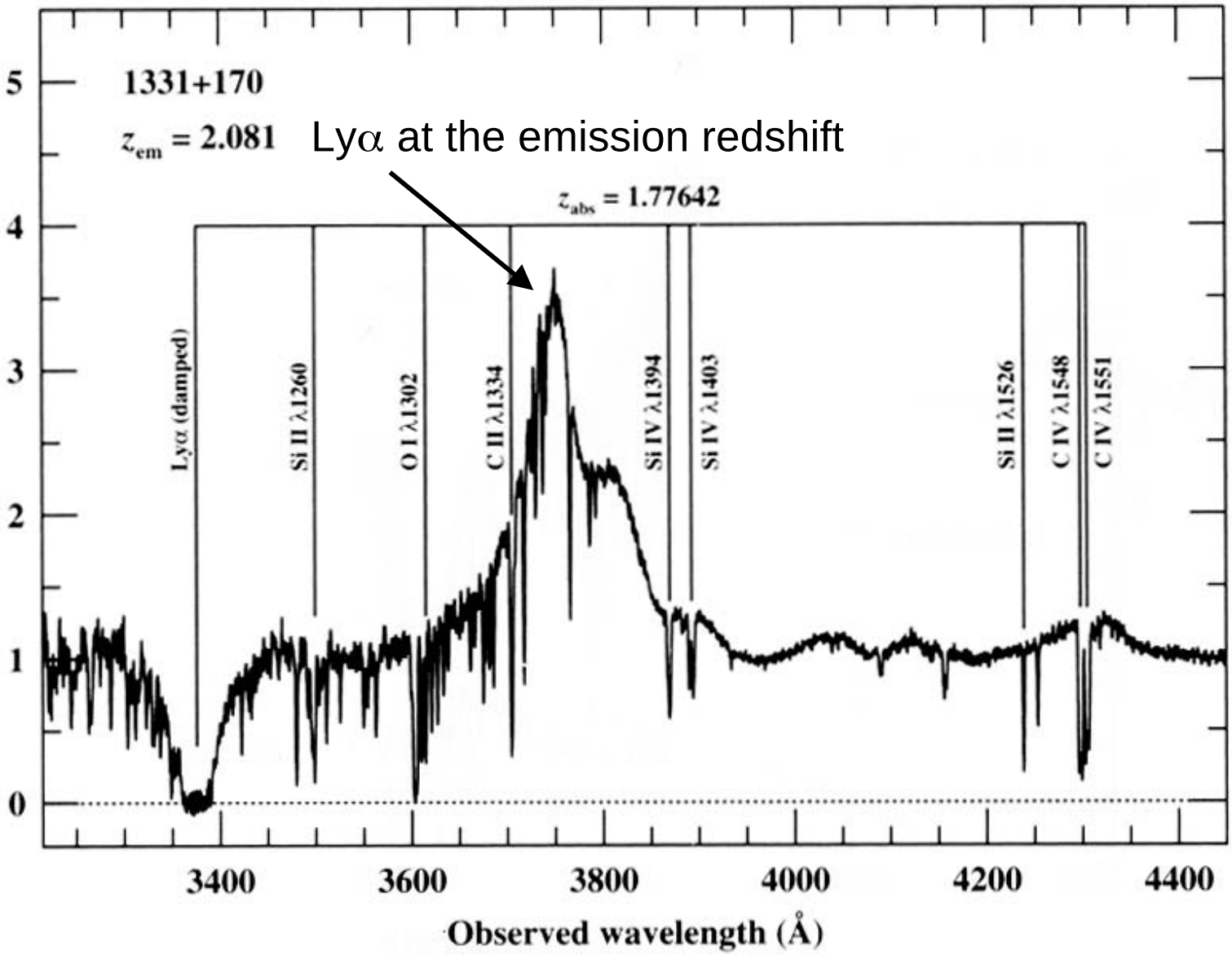

Marked lines are all at the same absorption redshift

Common Quasar Absorption Lines

Transition	Vacuum Wavelength (Å)
Lyman limit	911.753
Lyγ	972.537
Lyβ	1025.722
Lyα	1215.67
Si IV 1393	1393.755
Si IV 1402	1402.770
C IV 1548	1548.187
C IV 1550	1550.772
Fe II 2382	2382.765
Fe II 2600	2600.173
Mg II 2796	2796.352
Mg II 2803	2803.531

- CIV and Mg II are one-electron ions with strong UV doublet transitions

  $s_{1/2} \rightarrow p_{1/2}, p_{3/2}$

  with significant splittings, (unlike for atomic H).
- The doublets are a tell-tale signature for metal lines.

Missing data (last column): *A*- or *f*-values (see NIST)

Usefulness of High Resolution

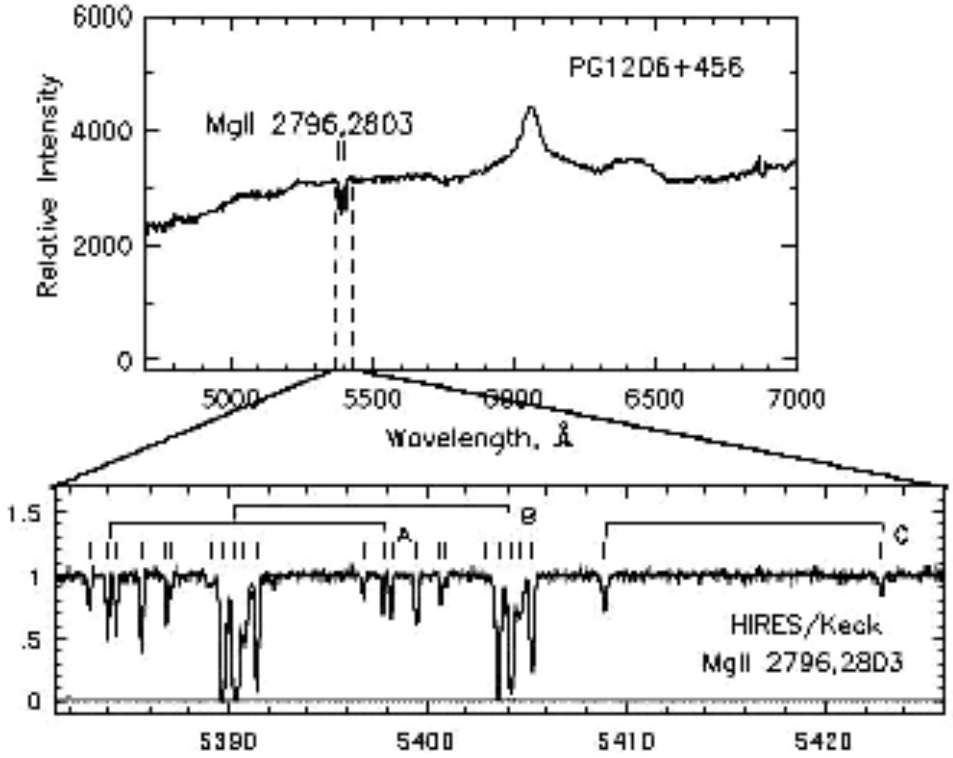

Top: *R* = 3000 spectrum of PG 1206+459 showing MgII 2796, 2803 absorption at ~ 5400 Å from a system at *z* = 0.927. ***Bottom:*** Kinematic structure is revealed at *R* = 45,000 with HIRES/Keck. Mg II 2796 Å is resolved into ~ a dozen components (5583-5592 Å), as is Mg II 2803 Å (5396-5406 Å), consisting of two clusters, *A* & *B*. A weaker Mg II doublet at *z* = 0.934 Å is labeled *C*. The line is a multiple Voigt-profile fit, with a cloud centered on each tick.

3. Observations of Absorption Lines

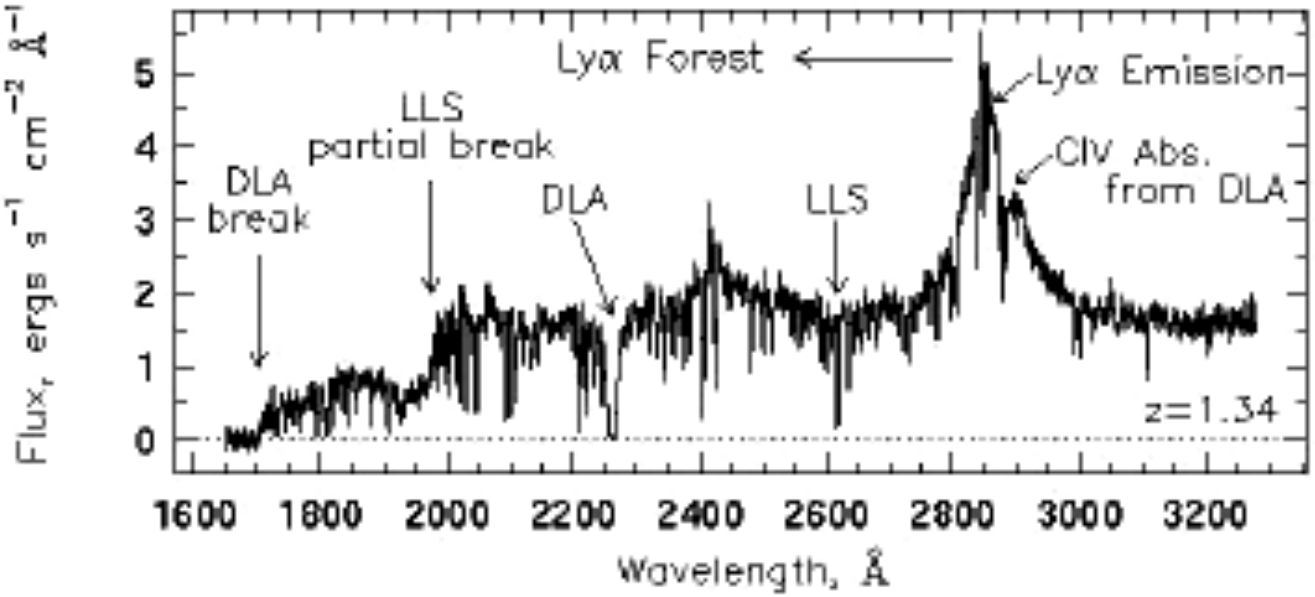

PKS 0454+0339, z_{em} =1.34 has several absorption systems

- In this example, the prominent emission lines are shifted by 2.34 to:
  Lyα - 2845, **Lyβ - 2400**, Lyγ- 2275, Ly_{cont}- 2133, CIV - 3625.
- There is a *Lyman Limit System* with redshift z = 1.15 and lines at
  Lyα - 2614, **Lyβ - 2205**, **Lyγ- 2090**, **Ly_{cont}- 1960**, CIV - 3330
- There is a *Damped* Lyα system with redshift z = 0.86 and lines at
  Lyα - 2261, **Lyβ - 1908**, **Lyγ- 1808**, **Ly_{cont}- 1695**, **CIV - 2881**

The profusion of narrow absorption lines is the Lyα forest

Absorption Line Systems

Each system has its own redshift z_{abs} and HI column N(HI). Since $z_{abs} < z_{em}$ and $\lambda_{obs} = (1+z)\,\lambda_0$, HI Ly$\alpha$ absorption systems form on the blue side of the quasar Lyα emission line where they form the Lyα Forest:

- log N(HI) < 17.2 - **Lyα Forest**, also with some lines of heavy elements
- 17.2 < log N(HI) < 20.3 - **Lyman Limit**

log N(HI) = 17.2 is just enough to make the Ly limit at 911.753 Å optically thick (σ_{phion}(H) = 6.3x 10^{-18} cm^{-2}). Similar to so-called metal line systems, where Lyα is unavailable.

- log N(HI) > 20.3 - **Damped Lyα Absorption** -

Large HI columns typical of gas-rich galaxies like the Milky Way.

Distribution of HI Absorbing Columns

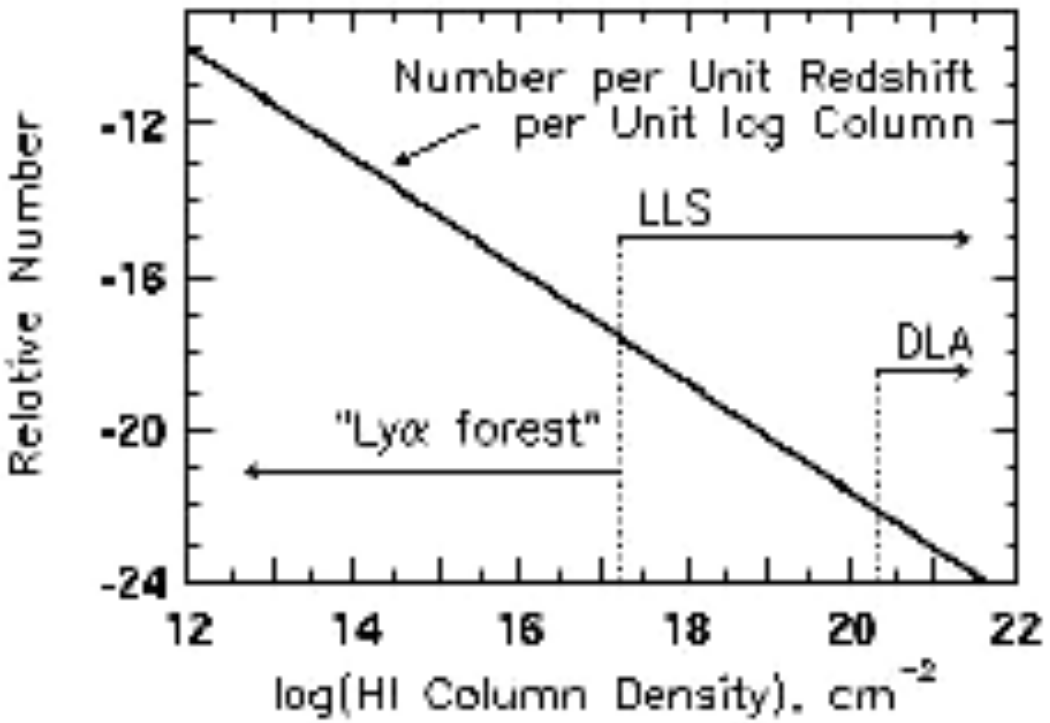

There are many more weak than strong lines.

Distribution in HI ~ N(HI)$^{-1.5}$

Evolution of The Lyα Forest

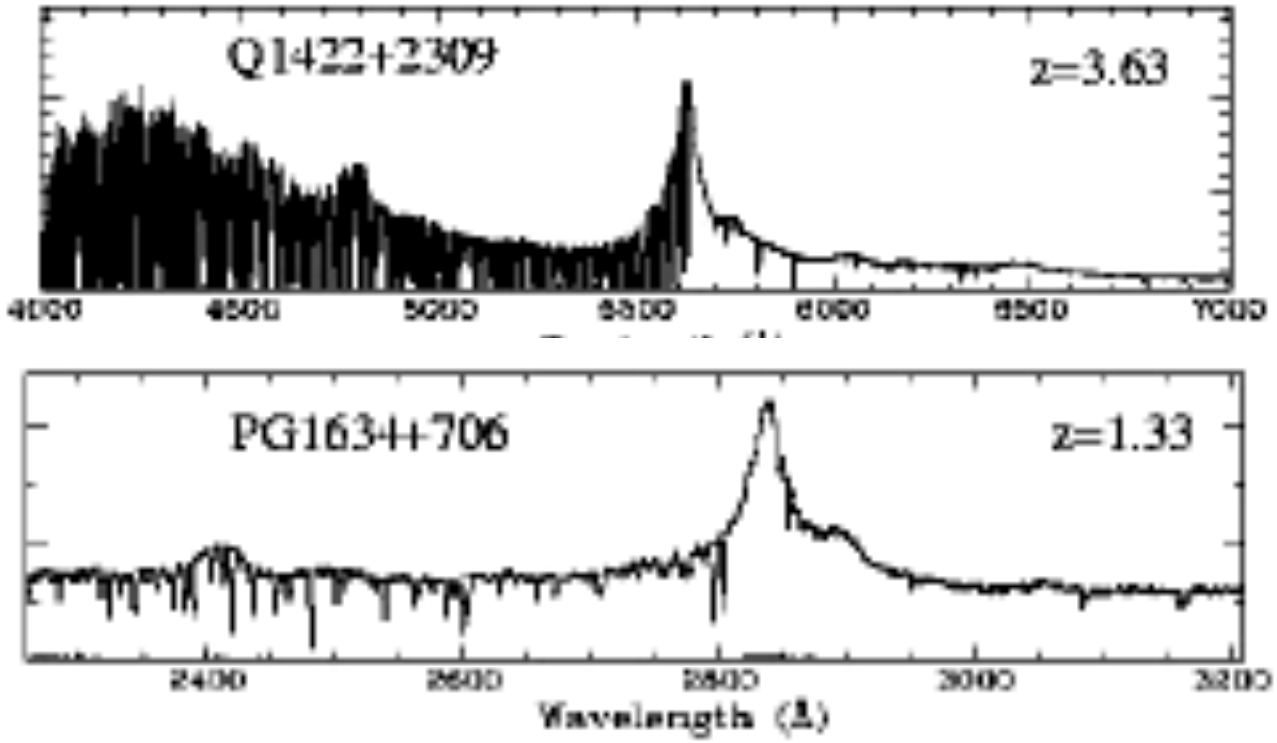

- The density of the forest increases with *z*
- Heavy element lines seem to be absent in high H-column absorbers indicating low "metallicities" 0.01 - 0.001 times solar even at *z* ~ 2

4. Damped Lyα Systems

Wolfe et al. ARAA 43 861 2005

- The spectra require sufficient HI columns to make the radiative (so-called damping) wings optically thick.
- The minimum (defining) HI column 2×10^{20} cm^{-2} is ~ same as nearby disk galaxies.
- This column is likely to be sufficient to shield the ambient ionizing radiation so that the clouds are largely neutral.
- The absorbing cloud may be a disk galaxy or a proto-galaxy.
- The Lyman Forest and Lyman Limit clouds are expected to be mainly ionized.
- Damped Lyα clouds are think enough to make measurements of heavy-element abundances
- Studying high-z Damped Lyα Systems is hampered by the thick Lyα Forest
- Research has been helped by the discovery of thousands of high-z quasars by the Sloan Digital Sky Survey (SDSS).
- Wolfe et al. review results for 600 Damped Lyα Systems

Two Damped Lyα Systems

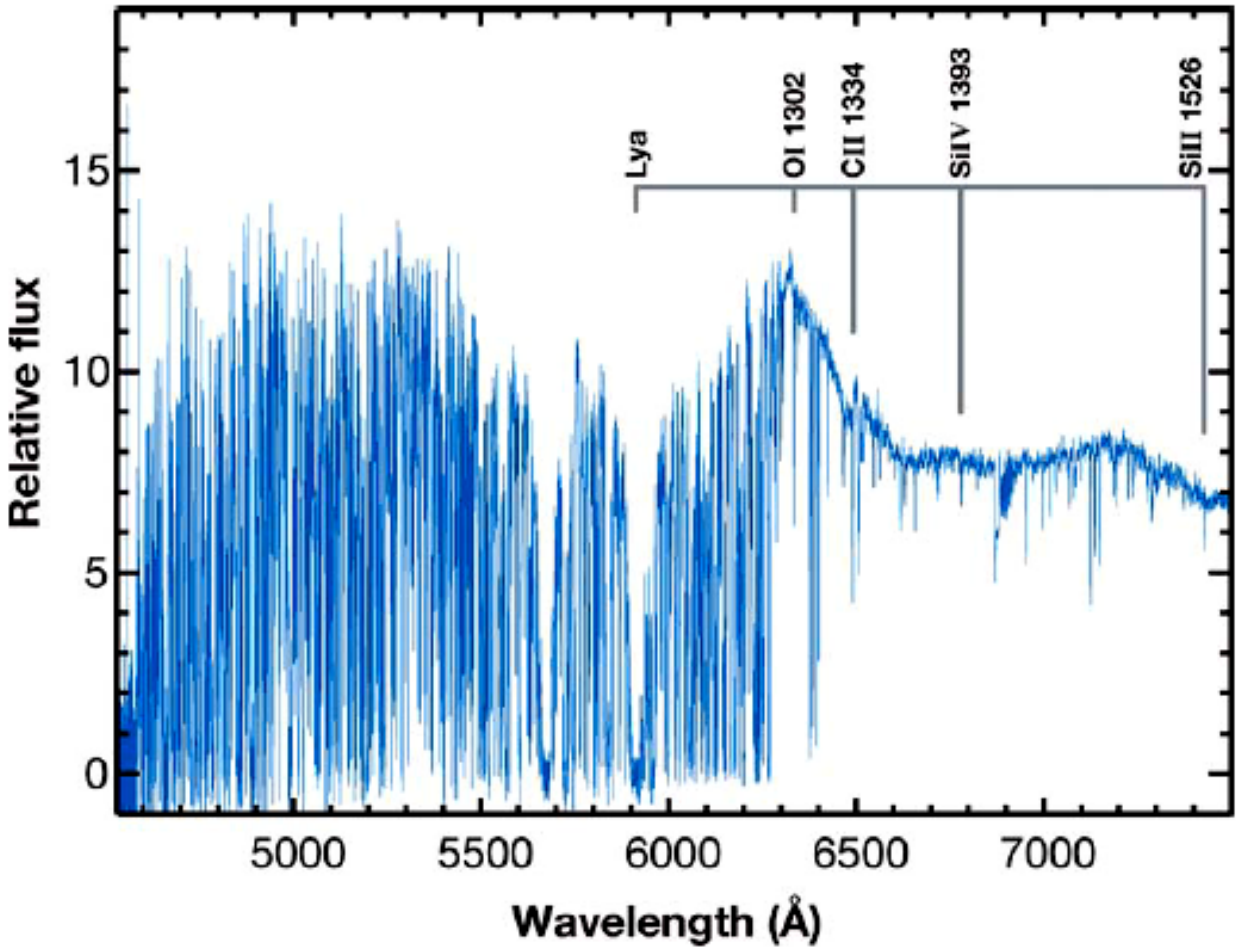

Figure 1 Keck/ESI spectrum of QSO PSS0209 + 0517 showing the Lyα forest, a pair of damped Lyα systems, and a series of metal lines. The schematic labeling in the figure identifies several key features for the damped Lyα system at $z = 3.864$. The absorption trough at $\lambda = 5674$ Å corresponds to the damped Lyα line at $z = 3.667$.

Voigt Profile Fits to Damped Lyα Features

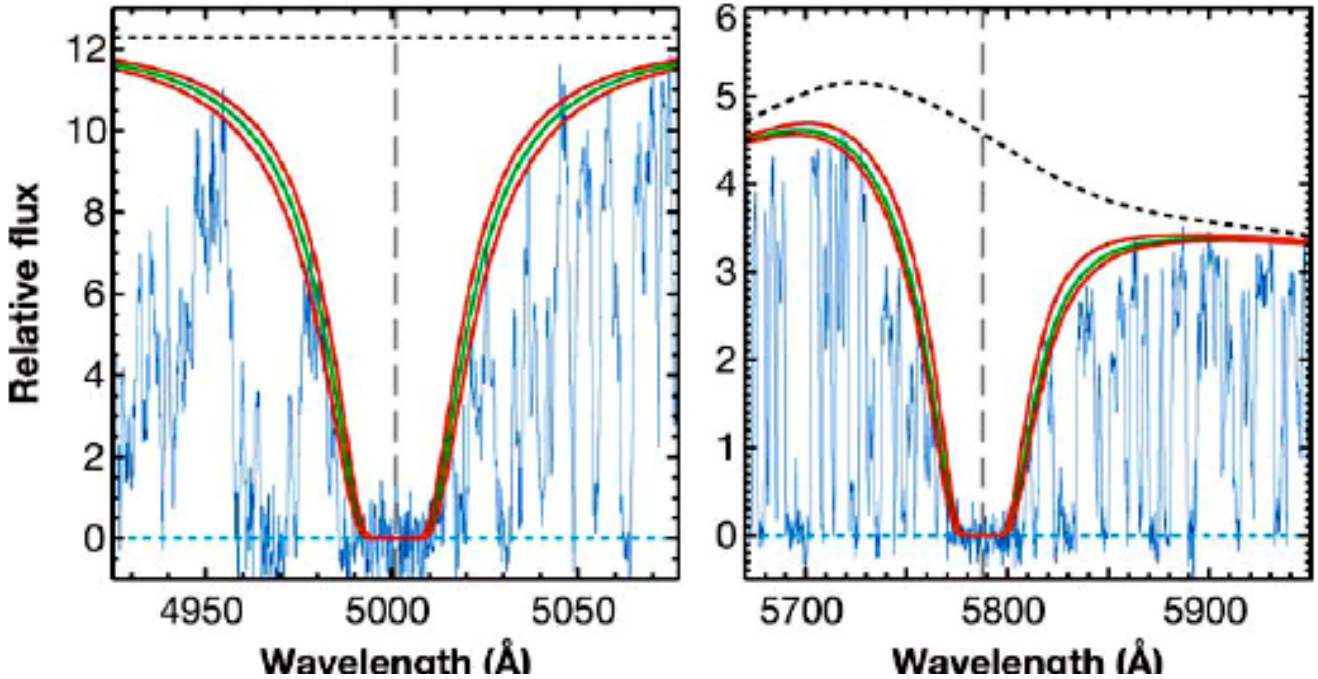

Fiugre 2 Example Voigt profile fits to two damped Lyα systems of the sample from Prochaska et al. (2003b). The vertical dashed line indicates the line centroid determined from metal-line transitions identified outside the Lyα forest. The dotted line traces the continuum of the QSO and the green and red lines trace the Voigt profile solution and the fits corresponding to 1σ changes to N(HI). The fluctuations at the bottom of the damped Lyα absorption troughs indicate the level of sky noise.

The high density of the Lyα forest complicates the analysis.
Here they are used to define a pseudo-continuum (dashed lines).

Fraction of Neutral Gas

• Focus on the binned data for the fraction of neutral gas Ω_g, normalized to the critical density, plotted vs. z.

• Notice the small uncertainties at z = 2.3, from which Wolfe conclude that Ω_g increases with z for large z.

The current fraction in stars is $\Omega_g = 2.5 \times 10^{-3}$. Much of the gas to make stars may have come from the Damped Lyα cloudss

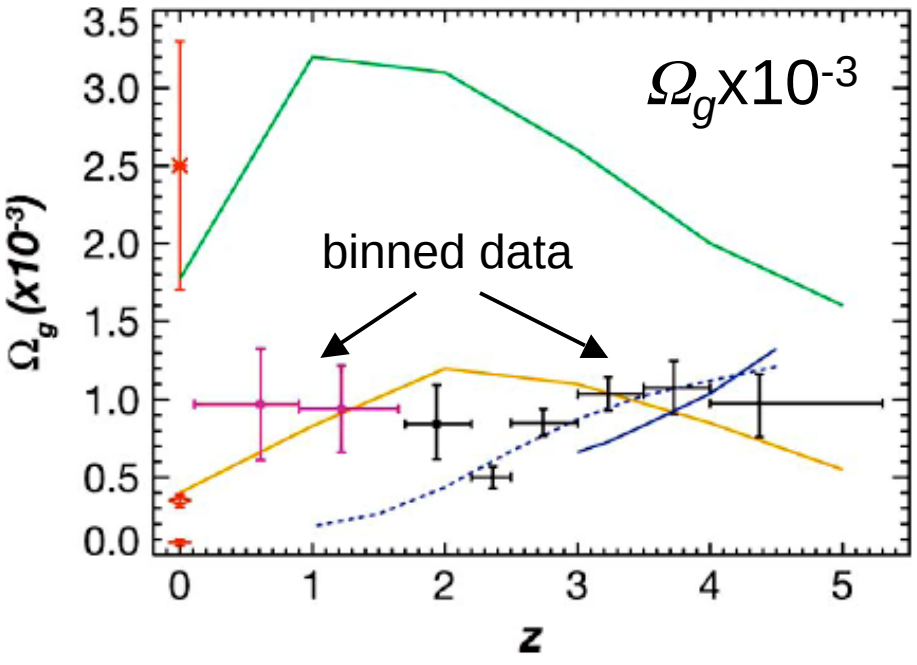

Figure 5 Neutral gas mass density versus z from Prochaska et al. (2005). H I data at (*a*) $z > 2.2$ from SDSS-DR3_4 survey, (*b*) $0 < z < 1.6$ from the MgII survey of S.M. Rao, D.A. Turnshek & D.B. Nestor (private communication), and (*c*) at $z = 0$ (*red diamond*) from Fukugita et al. (1998). Stellar mass density at $z = 0$ (*red star*) from Cole et al. (2001) and stellar mass density of Irr galaxies (*red plus sign*) from Fukugita et al. (1998). Theoretical curves from Cen et al. (2003) (*green*), Somerville et al. (2001) (*yellow*), and Nagamine et al. (2004a) (*blue*; *dotted* is D5 model and *solid* is Q5 model).

Measuring Abundances vs. Redshift

z=3.608

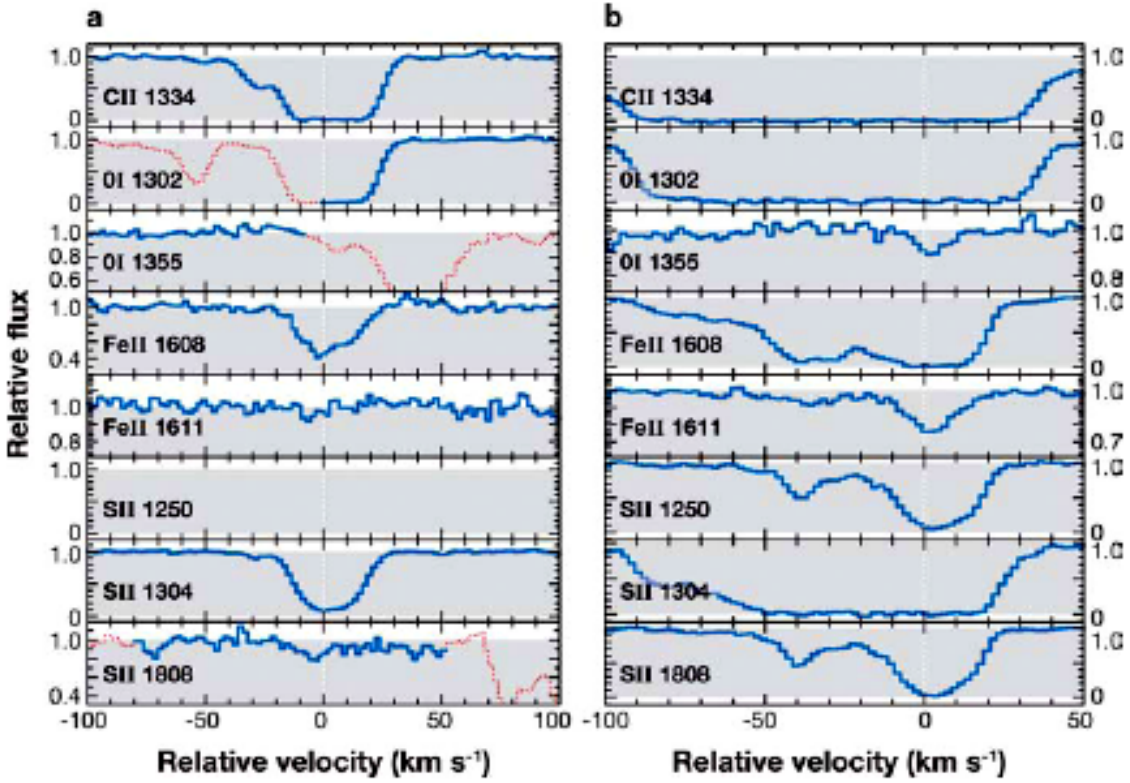

z=0.626

Figure 6 Velocity profiles of metal-line transitions for (*a*) the metal-poor damped Lyα system at $z = 3.608$ toward Q1108 – 07 and (*b*) the metal-strong damped Lyα system at $z = 2.626$ toward Q0812 + 32. *Gray* indicates the range of flux between 0 and 1. *Red lines* are blends due to other transitions.

Clear evidence that the metallicity decreases with z

Metallicity vs. Time

Binned data in green normalized to solar abundances, showing decrease by ~ 20 with z

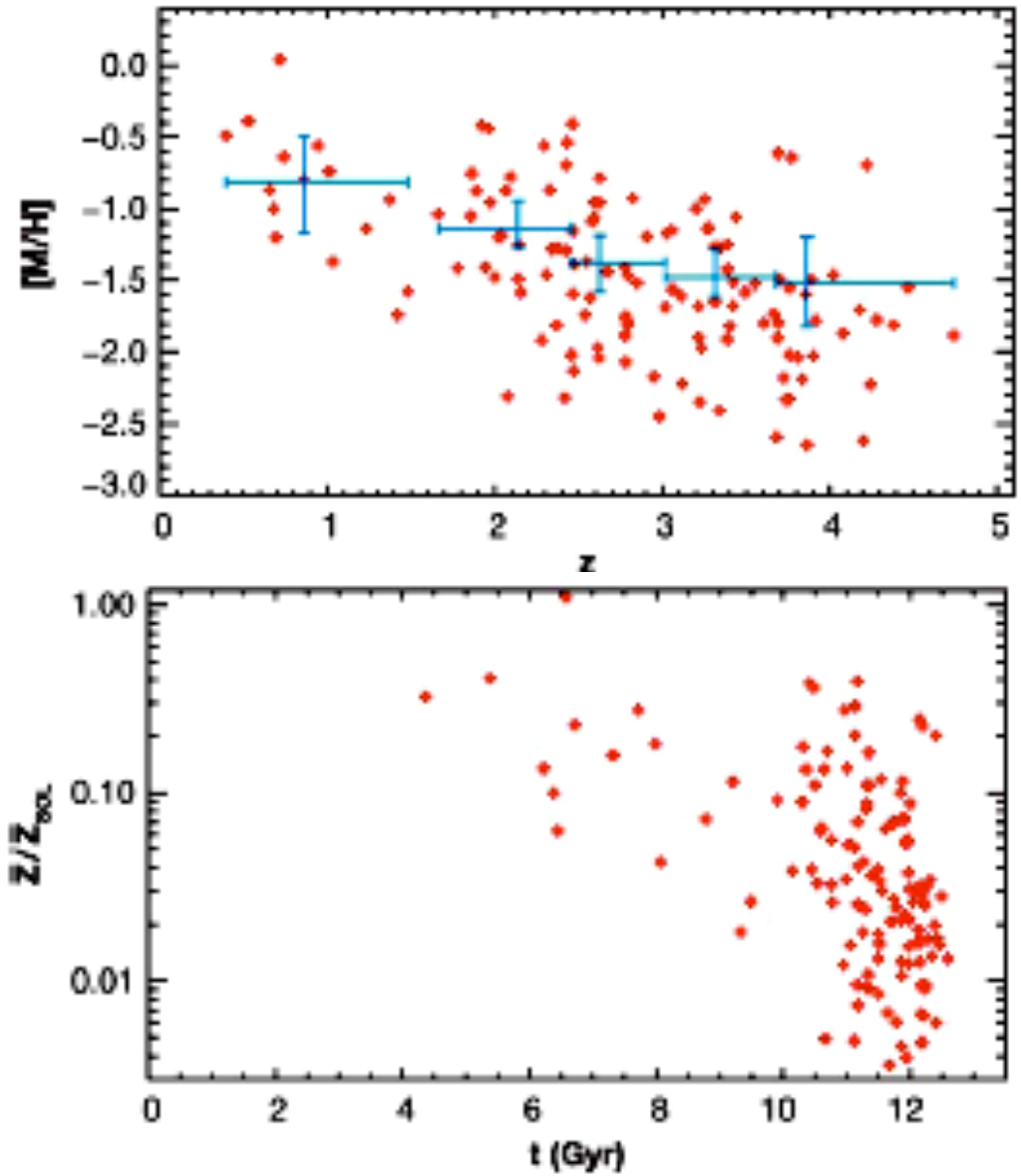

Most of the data are from > 10 Gyr

Dust in Damped Lyα Systems

Indirect Method: Ratio of little depleted Zn (slightly refractory) to highly depleted Cr or Fe (very refractory) - as in the local ISM.

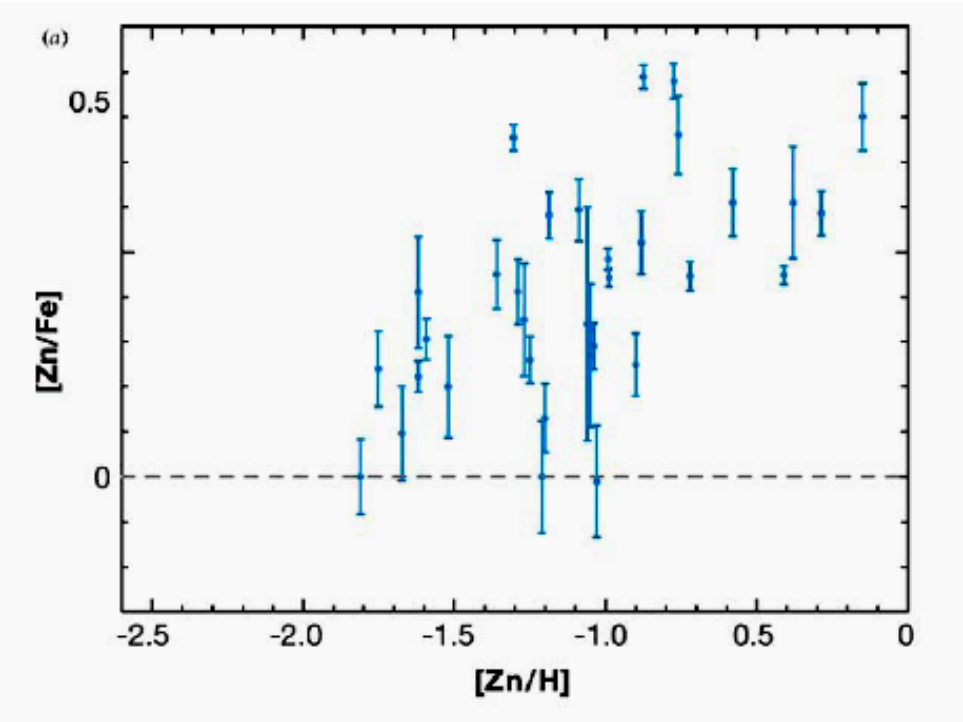

Zn/Fe vs. Zn/H increases with increasing metallicity as indicated by the abundance of Zn. Notice the range of metallicity seen in damped Lyα systems, symptomatic of a small dust-to-gas ratio.

NB Low metallicity may be partly responsible for the detection of only weak Lyman and Werner band absorption, suggesting $H_2/H \sim 10^{-3}$

Summary of Damped Lyα Systems

Main Results

- Contain most of the neutral gas in the redshift range z=0-5
- Some variation of the mass fraction with z; larger for large z than z=0
- Low metallicity (in the range -2.6 to -0.1)
- Evidence for dust from Zn/Fe ratio
- 20% have H_2

Problems and Questions

- Few identifications with other high-z galaxies, e.g., Lyman-break gaalaxies
- Detailed properties of the interstellar gas
- Star formation
- Galaxies vs. proto-galaxies
- Mass in dark-matter halos